The Journal of Engineering

*The 14th IET International Conference on AC and DC Power Transmission (ACDC 2018)*

IET Journals
The Institution of Engineering and Technology

# Dynamic interaction between synchronous machine and DC-power-modulated LCC in electromechanical timescale

eISSN 2051-3305
Received on 28th August 2018
Accepted on 19th September 2018
E-First on 6th February 2019
doi: 10.1049/joe.2018.8735
www.ietdl.org

*Jiazuo Hou[1], Shicong Ma[2], Xuan Gong[1], Jiabing Hu[1]* ✉

[1]*School of Electrical and Electronic Engineering, Huazhong University of Science and Technology, Wuhan 430074, People's Republic of China*
[2]*China Electric Power Research Institute (CEPRI), Beijing 100192, People's Republic of China*
✉ *E-mail: j.hu@hust.edu.cn*

**Abstract:** Active power modulation of line-commutated converter (LCC)-based high-voltage direct current (HVDC) system is increasingly utilised, especially for the case of damping low-frequency oscillation associated with synchronous machine (SM) in electromechanical timescale (around 1 Hz). Many papers have tried to analyse the mechanism of damping effects, but almost rely on numerical studies, which cannot reveal the dynamic interaction between SM and DC-power-modulated LCC. This study proposes a small-signal model of DC-power-modulated LCC based on motion equation concept. With this model, analytical investigation of low-frequency oscillation from the scope of damping and synchronising powers is presented. Comparisons of analytical results and eigenvalues draw some general conclusions which offer insight into the dynamic behaviour. By examining the case of an SM connected to a DC-power-modulated LCC, simulations in MATLAB/Simulink are conducted to verify the analytical results.

## 1 Introduction

Since active power modulation was successfully applied to the Pacific high-voltage DC current (HVDC) Intertie in 1976 [1, 2], DC modulation is increasingly used in modern power systems, which allows HVDC to have the ability to stabilise power system, including damping low-frequency oscillation by active power modulation.

As a result of lacking damping of electromechanical mode in power system, low-frequency oscillation usually occurs in electromechanical timescale (around 1 Hz), in which DC-power-modulated LCC with certain operation parameters can interact with synchronous machine (SM).

Many papers have tried to analyse the influences on low-frequency oscillation by active power modulation, but almost rely on numerical studies like eigenvalues [3, 4], which, though are effective to uncover some influential parameters' effects, are not intuitive enough to understand the dynamic interaction between SM and DC-power-modulated LCC.

Demello and Concordia [5] proposed an analytical method to analyse the dynamic interaction between torque–speed–angle loop in SM and the rest of power system based on the concepts of damping and synchronising powers. However, by packaging the rest of power system as a black box, how certain device in black box influences SM is unknown.

The contributions of this paper lie mainly in two aspects. Firstly, this paper proposes a small-signal model of DC-power-modulated LCC based on motion equation concept. By applying the modelling idea to other power electronic devices, the whole devices in power system can be modelled in a unified and modularised way, which provides a new perspective to analyse the dynamic interaction in multi-device power system. Secondly, this paper conducts an analytical investigation of low-frequency oscillation from the scope of damping and synchronising powers, which depicts the mechanism on how DC-power-modulated LCC influences SM.

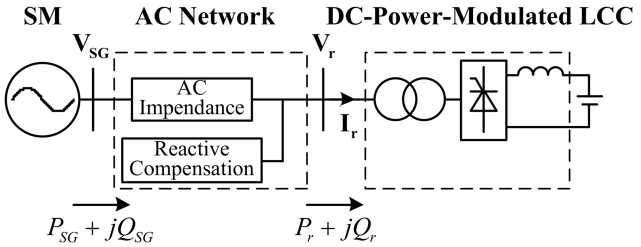


**Fig. 1** *Typical scenario to study the dynamic interaction between SM and DC-power-modulated LCC*

The rest parts of this paper are organised as follows. In Section 2, DC-power-modulated LCC HVDC system is modelled based on motion equation concepts. Section 3 presents a comprehensive analytical investigation between DC-power-modulated LCC and SM. Eigenvalue analysis and time-domain simulations are conducted in Section 4 to verify the above theoretical analysis. Finally, Section 5 draws the conclusion.

## 2 Modelling of DC-power-modulated LCC HVDC system

To analyse the dynamic interaction between SM and DC-power-modulated LCC, a typical scenario is chosen as illustrated in Fig. 1, where the power system is divided into three parts, i.e. an SM, a DC-power-modulated LCC rectifier, and a simple AC network.

It is noted that the dynamic of LCC inverter is neglected and replaced with an ideal DC voltage source to simplify the analysis, which is necessary for analytical investigation with relatively low complexity.

This section proposes small-signal models of the three parts illustrated in Fig. 1 based on motion equation concepts.

### 2.1 SM model based on motion equation concept

To simplify the dynamic interaction between SM and DC-power-modulated LCC, dynamics of SM is considered only characterised by rotor motion illustrated in Fig. 2 [6].

According to Fig. 2, SM model based on motion equation concept can be expressed as

$$\Delta\theta_{\mathrm{SM}} = G_{\mathrm{SM}}(s)\Delta P_{\mathrm{SM}} \tag{1}$$

where

$$G_{\mathrm{SM}}(s) = \frac{-\omega_b}{M_{\mathrm{SM}}s^2 + D_{\mathrm{SM}}s} \tag{2}$$

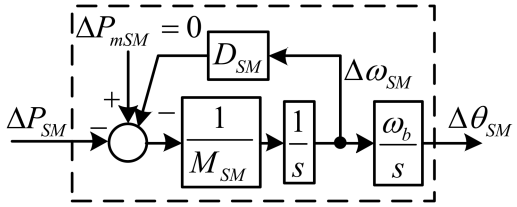


**Fig. 2** *Rotor motion of SM model*

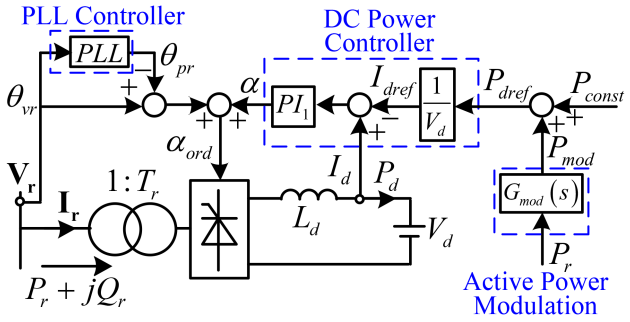


**Fig. 3** *Scheme of a DC-power-modulated LCC rectifier*

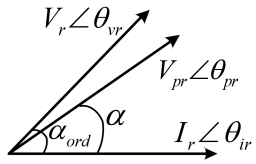


**Fig. 4** *Phase relationships of DC-power-modulated LCC*

Based on (1) and (2), it is noted that phase motion of SM is characterised by inertia coefficient $M_{SM}$ and damping coefficient DSM, while no dynamic is considered in magnitude motion.

### 2.2 Small-signal modelling of DC-power-modulated LCC

A number of simplifying assumptions are made to hold the main behaviour of concern of DC-power-modulated LCC model.

- Influences of commutation angle are neglected.
- Active power losses on converter transformer and thyristor are neglected.
- Dynamic of DC voltage $V_d$ is neglected.
- Converter transformer works on unsaturated situation.
- Harmonics in AC system are not taken into consideration.

Fig. 3 depicts a simplified diagram of LCC rectifier composed of DC-power controller, phase-lock loop (PLL) controller, and active power modulation.

*2.2.1 Linearisation of DC-power controller:* Neglecting the dynamic in DC voltage $V_d$, the firing angle $\alpha$ equation related to DC-power controller is given by

$$\alpha=\left(k_{p1}+\frac{k_{i1}}{s}\right)\left(I_d-\frac{1}{V_d}P_{dref}\right) \tag{3}$$

By linearising (3) at some initial operating point, there exists

$$\Delta\alpha=\left(k_{p1}+\frac{k_{i1}}{s}\right)\left(\Delta I_d-\frac{1}{V_d}\Delta P_{dref}\right) \tag{4}$$

*2.2.2 Linearisation of active power modulation:* The structures and parameters of active power modulation vary to meet different needs [7]. To damp low-frequency oscillation related to fluctuation of AC active power, active power modulation in this paper chose the variation of AC active power $P_r$ as input, and additional DC-power reference value $P_{mod}$ as output, so there exists

$$P_{mod}=G_{mod}(s)P_r \tag{5}$$

$$P_{dref}=P_{mod}+P_{const} \tag{6}$$

As illustrated in Fig. 3, the structure of active power modulation $G_{mod}(s)$ is designed as [8]

$$G_{mod}(s)=K_{mod}\left(\frac{1}{1+T_R s}\right)\left(\frac{1+T_1 s}{1+T_2 s}\right)^4 \tag{7}$$

Linearising (5) and (6) at some initial operating point yield

$$\Delta P_{mod}=G_{mod}(s)\Delta P_r \tag{8}$$

$$\Delta P_{dref}=\Delta P_{mod} \tag{9}$$

*2.2.3 Linearisation of PLL:* PLL's output phase can be expressed as

$$\theta_{pr}=\frac{1}{s}\left(k_{p2}+\frac{k_{i2}}{s}\right)\sin(\theta_w-\theta_{pr}) \tag{10}$$

Linearising (10) at some initial operating point yield

$$\Delta\theta_{pr}=\left(\frac{k_{p2}}{s}+\frac{k_{i2}}{s^2}\right)(\Delta\theta_w-\Delta\theta_{pr}) \tag{11}$$

*2.2.4 Linearisation of AC current's phase:* Neglecting the influences of commutation angle, the relationships of PLL's output phase $\theta_{pr}$, AC current's phase $\theta_{ir}$, and firing angle $\alpha$ are shown in Fig. 4, which can be written as

$$\theta_{ir}=\theta_{pr}-\alpha \tag{12}$$

By linearising (12) at some initial operating point, there exists

$$\Delta\theta_{ir}=\Delta\theta_{pr}-\Delta\alpha \tag{13}$$

*2.2.5 Linearisation of dynamic of smoothing reactance:* Neglecting the active power loss on converter transformer and thyristor, dynamic on smoothing reactance can be expressed as

$$P_r-P_d=\frac{1}{2}sL_dI_d^2 \tag{14}$$

Linearising (14) at some initial operating point yield

$$\Delta P_r-\Delta P_d=L_dI_{d0}s\Delta I_d \tag{15}$$

where subscript 0 represents initial values when linearising. It is noted that the dynamic of DC power $\Delta P_d$ is only determined by the dynamic of DC current $\Delta I_d$, which can be expressed as

$$\Delta P_d=V_d\Delta I_d \tag{16}$$

*2.2.6 Linearisation of AC current's magnitude:* Neglecting harmonics in AC system, the magnitude of the fundamental frequency component of root mean square value of AC current can be expressed as

$$I_r=\frac{\sqrt{6}T_r}{\pi}I_d \tag{17}$$

Linearising (17) at some initial operating point yield

$$\Delta I_r=\frac{\sqrt{6}T_r}{\pi}\Delta I_d \tag{18}$$

Based on (4), (8), (9), (11), (13), (15), (16), and (18), the corresponding small-signal model of DC-power-modulated LCC is illustrated in Fig. 5.

### 2.3 DC-power-modulated LCC model based on motion equation concept

Developed from basic rotor motion equation of SM, keys of motion equation concept lie on two aspects [9]. Firstly, dynamics of magnitude and phase of output variables are determined by the variation of active and reactive power input, which provide a physical perspective to depict the characteristics of magnitude and phase of output variable when unbalanced power input varies. Secondly, the model based on motion equation should only depend on the model's own parameters without the influences of other devices in the power system.

As shown in Fig. 5, the dynamic of DC-power-modulated LCC's output AC current is determined by variation of active power $\Delta P_r$ and phase of terminal voltage $\Delta\theta_{\mathrm{v}r}$. To replace $\Delta\theta_{\mathrm{v}r}$ with variation of active power $\Delta P_r$ and reactive power $\Delta Q_r$, it is noted that

$$P_r = V_{\mathrm{v}r} I_{\mathrm{i}r} \cos\varphi_r \tag{19}$$

$$Q_r = V_{\mathrm{v}r} I_{\mathrm{i}r} \sin\varphi_r \tag{20}$$

where $\varphi_r$is the power factor angle which are expressed as

$$\varphi_r = \theta_{\mathrm{v}r} - \theta_{ir} \tag{21}$$

Expressing (19) and (20) in terms of perturbed value yields

$$\Delta\theta_{\mathrm{v}r} = \Delta\theta_{ir} + k_1\Delta P_r + k_2\Delta Q_r \tag{22}$$

where

$$k_1 = -\frac{\sin\varphi_{r0}}{V_{\mathrm{v}r0} I_{r0}} \tag{23}$$

$$k_2 = \frac{\cos\varphi_{r0}}{V_{\mathrm{v}r0} I_{r0}} \tag{24}$$

By setting unbalanced active power $\Delta P_r$and unbalanced reactive power $\Delta Q_r$ as inputs, and setting AC current's magnitude $\Delta I_r$ and AC current's phase $\Delta\theta_r$ as outputs, characteristics of DC-power-modulated LCC is illustrated in Fig. 6, which are expressed as

$$\begin{bmatrix}\Delta I_r \\ \Delta\theta_{ir}\end{bmatrix} = \begin{bmatrix}G_{r11}(s) & 0 \\ G_{r21}(s) & G_{r22}(s)\end{bmatrix}\begin{bmatrix}\Delta P_r \\ \Delta Q_r\end{bmatrix} \tag{25}$$

To describe the model in the form of motion equation like (2), elements of matrix $\boldsymbol{G}_r(s)$ can be expressed as

$$G_{r11}(s) = \frac{1}{M_{r11}(s)s^2 + D_{r11}(s)s} \tag{26}$$

$$G_{r21}(s) = \frac{1}{M_{r21}(s)s^2 + D_{r21}(s)s} \tag{27}$$

$$G_{r22}(s) = \frac{1}{M_{r22}(s)s^2 + D_{r22}(s)s} \tag{28}$$

where inertial coefficients $M_{r11}(s)$, $M_{r21}(s)$, $M_{r22}(s)$ and damping coefficients $D_{r11}(s)$, $D_{r21}(s)$, $D_{r22}(s)$ are frequency-dependent, which is different from motion equation of SM.

Based on (25)–(28), it is noted that dynamics of DC-power-modulated LCC can be described as motions of magnitude and phase of AC current determined by variations of active and reactive power input. To be more precisely, magnitude motion is only determined by active power input, while phase motion is determined by both active power input and reactive power input.

Furthermore, from Fig. 6, it is interesting to find that magnitude motion of DC-power-modulated LCC is simply characterised by dynamics of smoothing reactance at certain operating point, while phase motion is mainly characterised by DC-power controller, PLL controller, active power modulation, and dynamics of smoothing reactance.

### 2.4 AC network model

In electromechanical timescale, dynamics of inductors and capacitors in AC network can be neglected, so AC network can be described as algebraic equations, which simplify the analytical investigation between SM and DC-power-modulated LCC. To establish a complete close loop of the studied power system, AC network is modelled as

$$\begin{bmatrix}\Delta P_{\mathrm{SM}} \\ \Delta P_r \\ \Delta Q_r\end{bmatrix} = \begin{bmatrix}H_{\mathrm{AC1}} & H_{\mathrm{AC2}} \\ H_{\mathrm{AC3}} & H_{\mathrm{AC4}}\end{bmatrix}\begin{bmatrix}\Delta\theta_{\mathrm{SM}} \\ \Delta I_r \\ \Delta\theta_{ir}\end{bmatrix} \tag{29}$$

where matrix $\boldsymbol{H}_{\mathrm{AC}}$ is determined by line inductance and reactive compensator.

## 3 Analytical investigation of dynamic interaction

This section first depicts two different influential paths between SM and DC-power-modulated LCC. Then the quantitative values of two paths are given by mathematical expressions

### 3.1 Influential paths between SM and DC-power-modulated LCC

Based on (25), (1), and (29), the corresponding model based on motion equation concept of Fig. 1 is illustrated in Fig. 7.

As illustrated in Fig. 7, SM's input power $\Delta P_{\mathrm{SM}}$ is influenced by two paths, viz. the direct influence from SM's output phase motion $\Delta\theta_{\mathrm{SM}}$, as well as the influence from DC-power-modulated LCC's magnitude motion $\Delta I_r$ and phase motion $\Delta\theta_{ir}$.

### 3.2 Quantitative values of influential paths

By substituting (25) into (29), equal feedback transfer function $F(s)$ of SM can be expressed as

$$\Delta P_{\mathrm{SM}} = F(s)\Delta\theta_{\mathrm{SM}} = \underbrace{F_1\Delta\theta_{\mathrm{SM}}}_{\Delta P_{\mathrm{SM1}}} + \underbrace{F_2(S)\Delta\theta_{\mathrm{SM}}}_{\Delta P_{\mathrm{SM2}}} \tag{30}$$

where

$$F(s) = \underbrace{H_{\mathrm{AC1}}}_{F_1} + \underbrace{H_{\mathrm{AC2}}\left(G_r^{-1}(s) - H_{\mathrm{AC4}}\right)^{-1}H_{\mathrm{AC3}}}_{F_2(S)} \tag{31}$$

From (31), it is noted that $F(s)$ is composed of two parts. Self-stabilising coefficient $F_1$ is only determined by AC network parameter, while en-stabilising coefficient $F_2(s)$ intuitively shows the quantitative dynamic interaction of DC-power-modulated LCC.

Moreover, it is noticeable that $F_1$ in electromechanical timescale is constant, while $F_2(s)$ in electromechanical timescale is frequency-dependent. In other words, $\Delta P_{\mathrm{SM1}}$ is completely in phase with $\Delta\theta_{\mathrm{SM}}$, which is a pure synchronising power, while $\Delta P_{\mathrm{SM2}}$ can be divided into two components, viz., synchronising power $\Delta P_{\mathrm{SM2}s}$ which is in phase with $\Delta\theta_{\mathrm{SM}}$, and damping power $\Delta P_{\mathrm{SM2}d}$ which is in phase with $\Delta\omega_{\mathrm{SM}}$, and can be expressed as

$$\Delta P_{\mathrm{SM1}} = F_1\Delta\theta_{\mathrm{SM}} \tag{32}$$

$$\Delta P_{\mathrm{SM2}}(s) = \underbrace{F_{2s}(s)\Delta\theta_{\mathrm{SM}}}_{\Delta P_{\mathrm{SM}\,2s}} + \underbrace{F_{2d}(s)\Delta\omega_{\mathrm{SM}}}_{\Delta P_{\mathrm{SM}\,2d}} \tag{33}$$

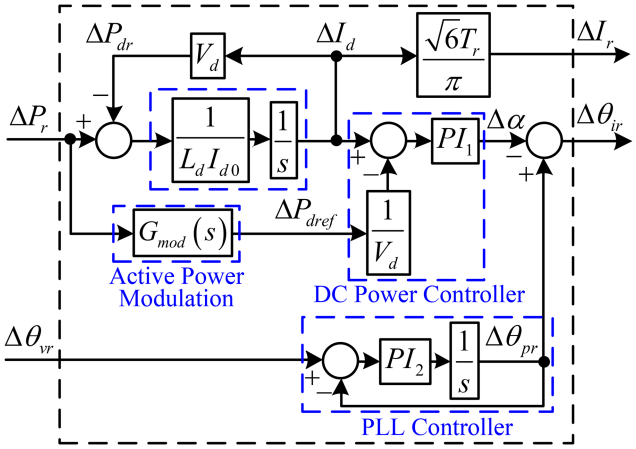


**Fig. 5** *Corresponding small-signal model of DC-power-modulated LCC of Fig. 3*

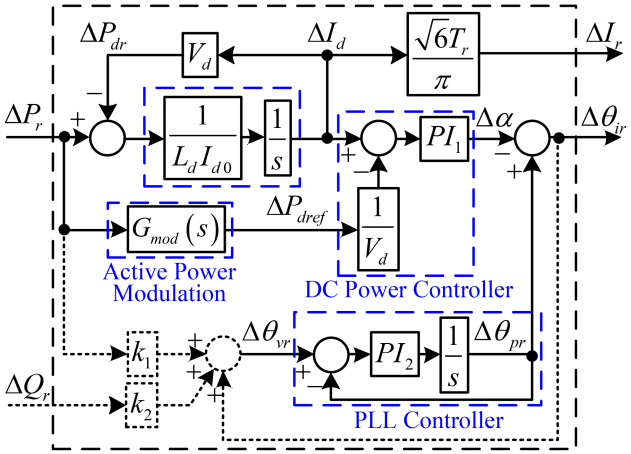


**Fig. 6** *Model of DC-power-modulated LCC based on motion equation concept*

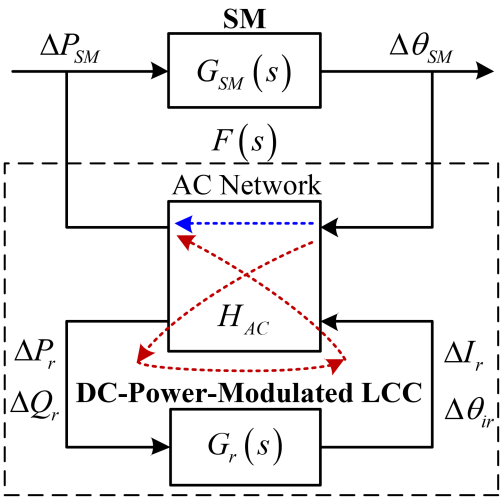


**Fig. 7** *Models of SM, AC network, and DC-power-modulated LCC based on motion equation concept*

Therefore, based on (30)–(33), dynamic interaction between SM and DC-power-modulated is illustrated in Fig. 8, where all the expressions of transfer functions are quantitative and intuitive in the forms of damping and synchronising powers

## 4 Verification

This section first verifies the proposed DC-power-modulated LCC model based on motion equation concept with the detailed model. Then analytical results of damping and synchronising powers are

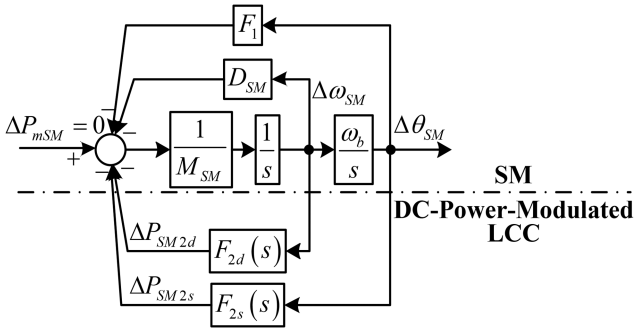


**Fig. 8** *Dynamic interaction between SM and DC-power-modulated LCC from the perspective of damping and synchronising powers*

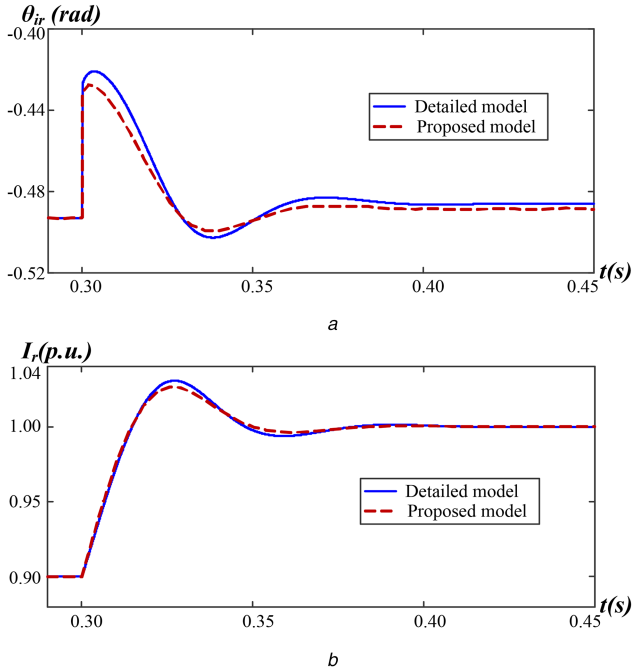


**Fig. 9** *Comparisons of simulation responses between the proposed and detailed models*
***(a)*** AC current's phase $\theta_{ir}$, ***(b)*** AC current's magnitude $I_r$

verified by the comparisons with eigenvalues and time-domain simulations in MATLAB/Simulink.

### 4.1 Verification of the proposed DC-power-modulated LCC model based on motion equation concept

To verify the phase and magnitude motion of the proposed DC-power-modulated LCC, a simple scenario shown in Fig. 3 is used, where DC-power-modulated LCC is connected to an infinite AC bus and an ideal DC voltage source.

Assuming that a small disturbance in DC-power reference value occurs at 0.3 s, Fig. 9 shows the comparative responses of AC current's phase $\theta_{ir}$ and AC current's magnitude $I_r$ between the proposed and detailed model. It is obvious that the proposed DC-power-modulated LCC is in good accordance with detailed model, which means the proposed model can hold the main behaviour in concerned electromechanical timescale.

### 4.2 Verification of the analytical results based on damping and synchronising power

The typical scenario shown in Fig. 1 is used to verify the analytical results. Generally, the structure and parameter of active power modulation are designed by pole placement technique [10]. As illustrated in Table 1, this paper designs two cases of different dominant poles by setting corresponding parameters of active power modulation.

**Table 1** Two cases of different dominant poles and corresponding parameters of active power modulation and calculated damping and synchronising coefficients

| | Case A | Case B |
|---|---|---|
| designed dominated poles | −0.5 ± j13.2 | −3.2 ± j13.2 |
| parameters of active power modulation | $K_{mod}$ = 0.0012 | $K_{mod}$ = 0.0025 |
| | $T_1$ = 0.26 | $T_1$ = 0.20 |
| | $T_2$ = 0.02 | $T_2$ = 0.03 |
| damping coefficient, p.u. | 0.1865 | 0.2893 |
| synchronising coefficient, p.u. | 0.0117 | 0.0120 |

**Table 2** Eigenvalue analysis of two cases in the proposed model

| | Eigenvalues | Response mode |
|---|---|---|
| Case A | | |
| $\lambda_{1,2}$ | −1.67 ± j13.18 | SM rotor |
| $\lambda_{3,4}$ | −0.50 ± j13.20 | active power modulation |
| $\lambda_{5,6}$ | −30.00 ± j22.37 | PLL control |
| $\lambda_7$ | −46.15 | DC-power control |
| $\lambda_8$ | −274.44 | smooth reactance |
| Case B | | |
| $\lambda_{1,2}$ | −1.67 ± j13.18 | SM rotor |
| $\lambda_{3,4}$ | −3.20 ± j13.20 | active power modulation |
| $\lambda_{5,6}$ | −30.02 ± j22.36 | PLL control |
| $\lambda_7$ | −46.15 | DC power control |
| $\lambda_8$ | −274.44 | smooth reactance |

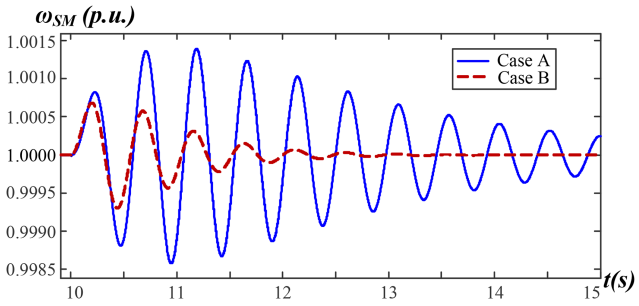


**Fig. 10** *Comparison of simulated responses of $\Delta\omega_{SM}$ in two cases*

Then, based on (32)–(33), damping and synchronising coefficients are calculated to reflect the dynamic interaction between SM and DC-power-modulated LCC. It is noticeable that small adjustment of active power modulation from case A to case B markedly improves the damping coefficient.

In addition, eigenvalues analyses of the proposed model of two cases are depicted in Table 2, and the related response mode are also given. It is worth mentioning that eigenvalues dominated by active power modulation are very close to eigenvalues dominated by SM rotor, while other eigenvalues are far away from these two. In other words, active power modulation in LCC can interact with SM in electromechanical timescale.

Also, time-domain simulations in MATLAB/Simulink are conducted to verify the analytical results. Assuming that a small disturbance in active power input $\Delta P_{SM}$, Fig. 10 shows the comparative responses of $\Delta\omega_{SM}$ in two cases. It is shown that oscillation frequencies of $\Delta\omega_{SM}$ are both 13.2 rad/s, while the attenuation speed of case B is much faster, which is in good accordance with analytical results.

## 5 Conclusion

Compared with voltage source converter and modular multilevel converter [11, 12], DC-power-modulated LCC plays an unique and fundamental role in damping low-frequency oscillation. This paper proposes a small-signal model of DC-power-modulated LCC based on motion equation concept, which is used for analytical investigation of low-frequency oscillation from the scope of damping and synchronising powers.

Compared with numerical studies, analytical investigation of dynamic interaction in this paper has two merits. On the one hand, based on the concept of motion equation, analytical study can directly show the paths between unbalanced power and magnitude/phase motion of devices, which can be easily applied to dynamic interaction among multi-device power system. On the other hand, from the scope of damping and synchronising powers, the effects of those paths are quantitative by mathematical expressions.

Besides, in order to damp low-frequency oscillation, it is suggested that the dominated poles of power system designed by active power modulation should be away from the left of the imaginary axis as well as the eigenvalues dominated by SM.

## 6 Acknowledgments

This work was supported in part by the National Key Research and Development Program of China under grant no. 2016YFB0900100, and Innovation Fund Project (XT83-17-002) of CEPRI.

## 7 References

[1] Cresap, R.L., Mittelstadt, W.A.: 'Small-signal modulation of the pacific HVDC intertie', *IEEE Trans. Power Appar. Syst.*, 1976, **95**, (2), pp. 536–541

[2] Cresap, R.L., Mittelstadt, W.A., Scott, D.N., *et al.*: 'Operating experience with modulation of the pacific HVDC intertie', *IEEE Trans. Power Appar. Syst.*, 1978, **PAS-97**, (4), pp. 1053–1059

[3] Grund, C.E., Pohl, R.V., Reeve, J.: 'Control design of an active and reactive power HVDC modulation system with Kalman filtering', *IEEE Trans. Power Appar. Syst.*, 1982, **PAS-101**, (10), pp. 4100–4111

[4] Smed, T., Andersson, G.: 'Utilizing HVDC to damp power oscillations', *IEEE Trans. Power Deliv.*, 1993, **8**, (2), pp. 620–627

[5] Demello, F.P., Concordia, C.: 'Concepts of synchronous machine stability as affected by excitation control', *IEEE Trans. Power Appar. Syst.*, 1969, **PAS-88**, (4), pp. 316–329

[6] Heffron, W.G., Phillips, R.A.: 'Effect of a modern amplidyne voltage regulator on underexcited operation of large turbine generators [includes discussion]', *Trans. Am. Inst. Electr. Eng. III, Power Appar. Syst.*, 1952, **71**, (1), pp. 692–697

[7] Guo, X.J., Ma, S.Y., Bu, G.Q., *et al.*: 'Present application situation of DC system participating in power system stability control and discussion on position of its functions in security defence system', *Dianwang Jishu/Power Syst. Technol.*, 2012, **36**, pp. 116–123

[8] Liu, H.F., Xu, Z.: 'Parameters tuning of HVDC small signal modulation controllers based on test signal'. 2003 IEEE Power Engineering Society General Meeting (IEEE Cat. No. 03CH37491), Toronto, Canada, 2003, vol. 4, p. 2531

[9] Yuan, H., Yuan, X., Hu, J.: 'Modeling of grid-connected VSCs for power system small-signal stability analysis in DC-link voltage control timescale', *IEEE Trans. Power Syst.*, 2017, **32**, (5), pp. 3981–3991

[10] Kundur, P.: '*Power system stability and control*' (McGraw-Hill, New York, 1994)

[11] Hu, J., Xiang, M., Lin, L., *et al.*: 'Improved design and control of FBSM MMC with boosted AC voltage and reduced DC capacitance', *IEEE Trans. Ind. Electron.*, 2018, **65**, (3), pp. 1919–1930

[12] Hu, J., Xu, K., Lin, L., *et al.*: 'Analysis and enhanced control of hybrid-MMC-based HVDC systems during asymmetrical DC voltage faults', *IEEE Trans. Power Deliv.*, 2017, **32**, (3), pp. 1394–1403